

Study on mechanical and microcrystalline on vinyl ester hybrid nanocomposites by WAXS

Shahryar Pashaei^a, Soleyman Hosseinzadeh^{b,*}, Basavarajaiah Siddaramaiah^c, R. Somashekar^d, Naser Ghorbani^a

^aDepartment of Chemistry, Payame Noor University, Tehran, Iran

^bDepartment of Chemical Engineering, Payame Noor University, Tehran, Iran

^cDepartment of Polymer Science and Technology, Sri Jayachamarajendra College of Engineering, Mysore, India

^dDepartment of Studies in Physics University of Mysore Manasagangotri, Mysore, India

Received: 14 October 2015, Accepted: 4 February 2016, Published: 4 February 2016

Abstract

The aim of this work is to probe the influence of nanoclay and turmeric spends content on microcrystalline of vinyl ester hybrid nanocomposites. A series of vinyl ester hybrid nanocomposites have been fabricated with varying amounts of turmeric spent (TS) viz., 0, 2.5, 5, 7.5 and 10 % w/w along with 2% nanoclay. The microcrystalline parameters such as crystallite size and lattice strain of vinyl ester hybrid nanocomposites have been measured by using wide-angle X-ray scattering (WAXS). These values were correlated with physico-mechanical properties of the vinyl ester hybrid nanocomposites with and without turmeric spent to understand the holistic behavior of the nanocomposites. Two prominent Bragg reflections at major peak in the 2θ region $17.35 - 17.79^\circ$ and a small shoulder in the 2θ region around $40.00-42.44^\circ$ were observed in the wide-angle X-ray diffraction patterns of the vinyl ester hybrid nanocomposites films of various ratios.

Keywords: hybrid nanocomposites; turmeric spent; microcrystalline; X-ray scattering.

Introduction

The use of natural fibers to reinforce polymers is a well-established practice,

and biocomposites are increasingly used in sectors such as automotive and construction. Green composites are a

*Corresponding author: Soleyman Hosseinzadeh
Tel: +98 (914) 1831109, Fax: +98 (44) 33855100
E-mail: hosseinzadeh65@gmail.com

specific class of bio-composites, where a bio-based polymer matrix is reinforced by natural fibers, and they represent an emerging area in polymer science [1]. Over the past years, sustainable eco-efficient practices and products have gained increasing attention and the use of natural fibers as reinforcement for polymers has been rapidly expanding [2-4]. In certain composite applications, biofibers have shown to be competitive in relation to glass fiber [5]. Advantages of biofibers over synthetic ones include the fact that they are renewable and biodegradable, present low cost, light weight, low energy consumption, carbon dioxide sequestration, low abrasiveness and excellent strength to weight ratio [6]. Limitations of biofibers as reinforcement in polymers are: difficulties in maintaining homogenization of fiber properties; processing temperature, which should not exceed the degradation temperature of these fibers of around 200 °C; and high moisture absorption, which may impair mechanical properties as well as facilitate fungus growth. Typical thermoplastic polymers that can be easily processed at temperatures up to 200-220 °C, and thus may be used as

matrix, include polypropylene (PP), polyethylene (PE), polystyrene (PS) acrylonitrile-butadiene-styrene (ABS), PVC and more recently polyvinyl butyral (PVB) [7].

In recent years, polymer/layered silicates nanocomposites have attracted great interest, both in industries and academia. Montmorillonite (Na-MMT) is commonly used as a nanofiller in the preparation of polymer nanocomposite. The possible application of generated organoclay is the better intercalation of polymer chains between stacks of MMT clay. The modified Na-MMT is used for making eco-friendly polymer clay nanocomposite with improved physical and mechanical properties. Montmorillonite, and other layered Polymer composites have been widely used for several years and their market share is continuously growing. It is widely known that the use of a polymer and one (or more) solid fillers allows obtaining several advantages and, in particular, a combination of the main properties of the two (or more) solid phases. Among the fillers used, calcium carbonate, glass fibers, talc, kaolin, mica, wollastonite, silica, graphite, synthetic fillers (e.g. PET- or PVA-based fibers), high performance fibers

(carbon, aramidic, etc) are worth citing [8].

In response to the new challenges, the authors are reporting the use of turmeric spent (TS) A as filler in fabrication of hybrid nanocomposites, because over 95 % of the TS are considered as waste after the extraction of curcumin, a nutraceutical which is in high demand in western countries. Consequently, the E-factor, a metric used for “greenness” [9] of the process, which is defined as “ratio of the total weight of waste produced to the total weight of the product obtained” assumes paramount importance. The objective of this research is the influence of o-MMT and TS content on mechanical and microstructural parameters such as crystallite size and lattice strain was determined using paracrystalline modeling of X-ray data.

Experimental

Materials

The resin used to prepare composite was general purpose vinyl ester, VRP-2121, obtained from M/s Vikram Polymers and Resins, Bangalore, India. The typical properties of vinyl ester are viscosity 650 cP at 25 °C and specific gravity 1.125 at 25 °C. Methyl ethyl ketone peroxide (MEKP) was used as

catalyst and cobalt octoate as promoter, and these were procured from M/s Sd fine Chemicals, Bangalore, India. Organically modified montmorillonite (Nano-mer I.31PS) was obtained from Sigma, Bangalore. It is surface modified MMT clay: (Na)- modifiers- gamma-aminopropyl triethoxysilane, octadecylamine (cation exchange capacity (CEC) ~145 meq/100 g) (MMT). Turmeric spent A (TS) (moisture content 6.4%, bulk density 1.32 g cm⁻³ and ash content 3.36% was obtained from M/s. Sami Labs, India as gift sample. All other chemicals used in this study are analytical reagent (AR) grades.

Filler Preparation

The TS was thoroughly washed with water to remove sand and other foreign impurities adhered on filler surface, dried in sunlight, and ground to fine powder of it, particles size of <240 μm. This fine powder was dried again in hot oven with air circulation for 24 h at 60 °C and stored in desiccators in sealed polyethylene covers until further use.

Preparation of hybrid nanocomposites

Nanoclay and TS filler loaded vinyl ester resin hybrid nanocomposites have been prepared by using in-situ polymerization

method. In this investigation, nanoclay and turmeric spent A were swollen in vinyl ester resin. Different amounts viz., 0, 2.5, 5, 7.5 and 10 wt. % of turmeric spent A (agro waste) along with 2 wt. % of o-MMT were mixed with the vinyl ester resin by means of a mechanical stirrer for 2 h at room temperature to obtain a homogenous mixture. Upon completion of degassing, the vacuum was released, MEKP and cobalt octoate were added at a ratio of 100:1.4:1.4 (resin: MEKP: cobalt octate) by weight while stirring slowly. The liquid mixture was then cast in a preheated cleaned and releasing agent smeared moulds and cured at room temperature for 24 h. To ensure complete curing, the composite and matrix sheets were post cured at 80 °C for 4 h. The post cured vinyl ester composite laminates were left in the oven and allowed to cool gradually to ambient temperature before removal from the moulds. The cured vinyl ester laminates were machined into different specimens as per ASTM specification for characterization by different methods [10].

Characterization

Swelling behavior

Procedure to measure percent swelling of composites in organic solvents is briefly explained as follows: a known weight (w_1) of dried hybrid nanocomposites was immersed in different solvents until a state of equilibrium was attained at room

temperature. When material swells, weight of the swollen material is noted (w_2). The percentage of swelling was calculated by the relation [11];

$$\text{Percentage swelling} = \frac{W_2 - W_1}{W_1} \times 100 \quad (1)$$

Wide angle X-ray scattering spectroscopy

Wide angle X-ray scattering (WAXS) data for the composites were recorded by Philips PW 1140 diffractometer with (35 mA, 30 KV) Bragg Brentano Geometry (fine focus setting) using Germanium monochromated radiation of Cu K ($\lambda = 1.5418\text{\AA}$), 2θ ranges from 5 to 50° using a curved position sensitive detector (CPSD) in the transmission mode. These patterns were indexed using TREOR procedure. The intensity was corrected for Lorentz-polarization factors and also instrumental broadening using Stoke's deconvolution method [12].

Microstructural parameters such as crystal size ($\langle N \rangle$) and lattice strain (gin %) are determined by using single order method, which is based on the Fourier method of Warren and Averbach in which the simulated intensity profile was matched with the experimental one [13, 14].

Fourier coefficient of Bragg reflection intensity profile is;

$$A(n) = \sum_{s=-\frac{s_0}{2}}^{+\frac{s_0}{2}} I(s) \cos[2fnd(s - s_0)] \quad (2)$$

Fourier coefficient A (n) is functions of crystallite size ($A_s(n)$) and disorder ($A_d(n)$) coefficients of the lattice. Here, $s = \sin \theta / \lambda$ and $d = [d_{hkl}]$ is lattice spacing. The Fourier coefficient can be written as;

$$A(n) = A_s(n) \cdot A_d(n) \quad (3)$$

$P(i)$ as the probability distribution function of column lengths, the size Fourier coefficient is as [15];

$$A_s(n) = 1 - \frac{nd}{D} - \frac{d}{D} \left[\int_0^n iP(i)di - n \int_0^n P(i)di \right] \quad (4)$$

where, $D = \langle N \rangle d$ is the crystallite size. Essentially, several asymmetric functions for $P(i)$ in equation (4) can be used to find the microstructural parameters. Using asymmetric exponential distribution function,

Somashekar et al [16] have arrived at the following expressions;

$$P(i) = \begin{cases} 0 & \text{if } p < i \\ r \exp\{-r(i - p)\} & \text{if } p \geq i \end{cases} \quad (5)$$

where, $r = 1/(N - P)$. Substituting eqn (4) in eqn (3) we get;

$$A_s(n) = \begin{cases} A(0) & \text{if } n \leq p \\ A(0) \exp\{-r(n - p)\} / (rN) & \text{if } n \geq p \end{cases} \quad (6)$$

With Gaussian probability distribution (21) function for the lattice strain coefficient

$A_d(n)$, we have;

$$A_d(n) = \exp(-2f^2 m^2 n g^2) \quad (7)$$

where, $g = d/d$ is the standard deviation of distribution of lattice vectors to their mean length, which is the parameter used to describe paracrystallinity. Initial values of $\langle N \rangle$ and 'g' were obtained using the method of Nandi et al [17] and then these values are refined. The surface weighted crystallite size values are computed using well-established procedure [18]. Required source code for computation has been written in FORTRAN language.

Results and discussion

Chemical resistance

The influences of chemical reagents such as acid, alkalies, water and hexane on the vinyl ester hybrid nanocomposite specimens have been measured and the obtained results are shown in Table 1. From the table, it was noticed that, the unfilled and TS filled vinyl ester hybrid

nanocomposites showed good resistance to acids. Percentage swelling in hexane media of bare vinyl ester is high as compared to filled vinyl ester hybrid nanocomposites. This result clearly indicates that resistance to the organic solvents increases with decrease in TS content in vinyl ester matrix.

Table 1. Chemical resistivity of chemical reagent filled vinyl ester

TS content in VE (wt. %)	10 % CH ₃ COOH	10 % HCl	10 % H ₂ SO ₄	10 % NaOH	10 % Na ₂ CO ₃	10 % NH ₄ OH	C ₆ H ₁₄
0	0.59	0.55	0.47	0.46	0.70	0.52	0.33
2.5	0.43	0.50	0.43	0.41	0.42	0.46	0.07
5	0.93	0.71	0.69	0.89	0.87	0.93	0.16
7.5	0.94	0.74	0.74	0.95	0.86	0.96	0.18
10	1.25	0.99	0.87	1.27	0.95	1.42	0.19

Water uptake behavior

Water absorption properties of any material are very important for design and optimization of many processes such as drying, packaging and storage. Water uptake, in case of polymer composites, depends on the nature of matrix and reinforcement and their compositions. Turmeric spent A is naturally occurring filler and being hydrophilic in nature. There is a need to address the water absorption behavior of TS incorporated hybrid nanocomposites to make it suitable for barrier application. The measured

equilibrium water uptake content is used to predict the hygroscopic nature of the composites. The equilibrium water uptake behavior is an important quantitative measure in the practice of moisture sensitive products or the final products which are come in contact with water.

The percentage water uptake for all TS filled nanocomposites, as a function of time, is shown in Figure 1. From the figure, it was noticed that, there was a gradual increase in weight for all systems with duration of exposure. There was no noticeable change in

water uptake behavior for the composites exposed above 3 days.

The composites with 10% TS content showed a steep increase in water uptake as compared to lower dosage of TS loaded nanocomposites (Figure 1). This is due to moisture sensitivity nature of TS filler. The water absorption behavior of the TS filled composites is mainly because of the presence of the lignocellulosic filler, since the polar vinyl ester absorbs no or little water. All the composites showed uptake of water which increases with increase in filler content and are attributed to the presence of lignocellulosic TS filler in the green composites. Because of the hydrophilic

nature of the agro-residues, the water tends to retain in the inter fibrillar space of the cellulosic structure of these fillers as well as flaws at the interface and micro voids present in the composites. In 2.5% turmeric spent with 2% of nanoclay, it showed lower than all green composites due to interaction between bear vinyl ester and nanoclay. Percentage of water absorption values clearly indicates that, vinyl ester green composites are more sensitive to water absorption as compared to pristine vinyl ester. The presence of water in the specimen reduces the performance of the composites. This is due to absorbed act as plasticizer in the polymer matrix.

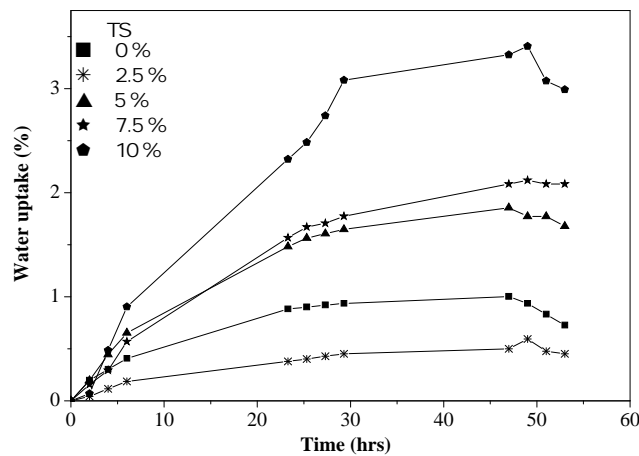


Figure 1. Percentage of water uptake of hybrid nanocomposites with various TS content at room temperature

The change in thickness of the composites also follows the same trend as explained above. The percentage change of thickness of the TS filled

nanocomposites increases with increase in duration of exposure as expected. From the study, it was noticed that the water uptake behavior strongly depends

upon the duration of exposure and TS content in composite systems.

Wide-angle X-ray scattering (WAXS) diffractogram

To probe the microstructure of nanoclay and TS filled vinyl ester hybrid nanocomposites, the powder x-ray diffraction patterns of the composites were recorded. X-ray diffractograms for 0 %, 2.5 %, 5 %, 7.5 % and 10 wt % TS filled hybrid composites are shown in Figures 2 (a)-(e). From the figure, it was noticed that there was broad and major peak in the 2θ region $17.35 - 17.79^\circ$ and a small shoulder in the 2θ region around $40.00 - 42.44^\circ$. It is evident from the figure that with the increase in o-MMT content, the peak shape and size in the 2θ region varied.

Figure 2 indicates that there is a broadening of reflection, which arises due to two main factors. The micro defects such as variation in crystal size ($\langle N \rangle$) and strain (g , in %) are responsible for broadening of the X-ray reflection in polymers [19]. Along with this, there is also a lattice disorder of a second kind known as paracrystallinity and normally this is quantified as strain ($g = \Delta d/d$), where 'd' is the interplanar spacing. The values of $\langle N \rangle$ and lattice

strain 'g' are the governing factors for the broadening of X-ray pattern. The variations in these microcrystalline parameters in nanocomposites can be attributed to change in molecular ordering and morphology with compositions.

The microcrystalline parameters such as the interplanar spacing (d_{hkl}), nanocrystal size ($\langle N \rangle$) measured in the direction perpendicular to Bragg (hkl) plane, lattice strain (g in %), and surface weighted crystal size (D_s) for the nanocomposites were calculated using exponential asymmetric distribution function and the results are given in Table 2.

Microstructure encompasses grain size, shape and the distribution functions of the grain-size parameters. Increase in o-MMT content did not show much variation in lattice strain, (g , in %); it was almost constant. Furthermore, a slight variation in number of unit cells ($\langle N \rangle$) and D_s values are with the compositions of the composites. But there was no systematic variation in $\langle N \rangle$ and D_s with reference to the compositions of the composites. Moreover, higher values of $\langle N \rangle$ and D_s were noticed for 5 wt. % loading in nanocomposite

systems. The change in $\langle N \rangle$ and D_s values indicates that the order of structure of the nanocomposites changes after incorporation of o-MMT.

The interplanar (d_{hkl}) distances of the first and second main peaks lie in the range of 4.98-5.25 and 2.12-2.25 respectively and a slight variation in d_{hkl} values with the composition of the composites. This implies that there is a change in the structure of the nanocomposites.

In order to know the most suitable asymmetric distribution, fitness test was conducted using line profile simulation from the peak of the reflection to its baseline. The experimental and simulated X-ray profiles for all composites were

calculated using both of the distribution functions. For the sake of comparison, specimen profiles obtained from exponential distribution function for 0%, 1%, 3% and 5 wt% o-MMT filled nanocomposites are shown in Figures 3 (a) – (d) respectively. It was evident from these figures that there is a good agreement between the experimental and theoretically calculated X-ray profiles. In all cases, it was noticed that the goodness of the fit was less than 10%. It is evident from this figure that the experimental data and the model parameters based on exponential distribution function are quite reliable. These methods for obtaining microstructural parameters were also reliable in other systems [20].

Table 2. Microstructural parameters of vinyl ester/o-MMT/TS green composites calculated employing exponential distribution function

TS content in nanocomposite	2 (deg)	d (Å)	$\langle N \rangle$	g (%)	*	$D = \langle N \rangle \cdot d$ (Å)
0	17.52	5.05	2.11	0.10	0.105	10.65
	40.69	2.21	3.33	0.10	0.166	07.35
2.5	17.65	5.02	2.23	0.10	0.111	11.19
	40.00	2.25	3.16	0.10	0.158	07.11
5	17.51	5.06	2.24	0.50	0.56	11.33
	41.61	2.16	3.33	0.10	0.166	07.21
7.5	17.79	4.98	1.98	0.10	0.099	09.86
	41.20	2.18	3.34	0.10	0.167	07.28
10	17.35	5.25	3.33	0.10	0.166	17.5
	42.44	2.12	2.91	0.10	0.145	06.16

According to Hosemann's model, these changes in crystal size values as well as shape ellipsoids are attributed to the interplay between the strains present in the polymer network. Also, the number of the unit cells coherently contributes to the X-ray reflection. This concept has been quantified in terms of the parameter, δ , called enthalpy. From $\langle N \rangle$ and g parameters, δ is calculated using Hosemann's paracrystalline disorder model [21]:

$$\delta = \langle N \rangle^{1/2} g$$

Table 2 indicates that the lower average values of δ (0.099 - 0.56) is in agreement with Hosemann's observation for the nanocomposites and the value represents the amount of energy needed for the formation of the polymer network. The phase stabilization in vinyl ester/o-MMT/TS composites has been quantified in terms of parameter, δ .

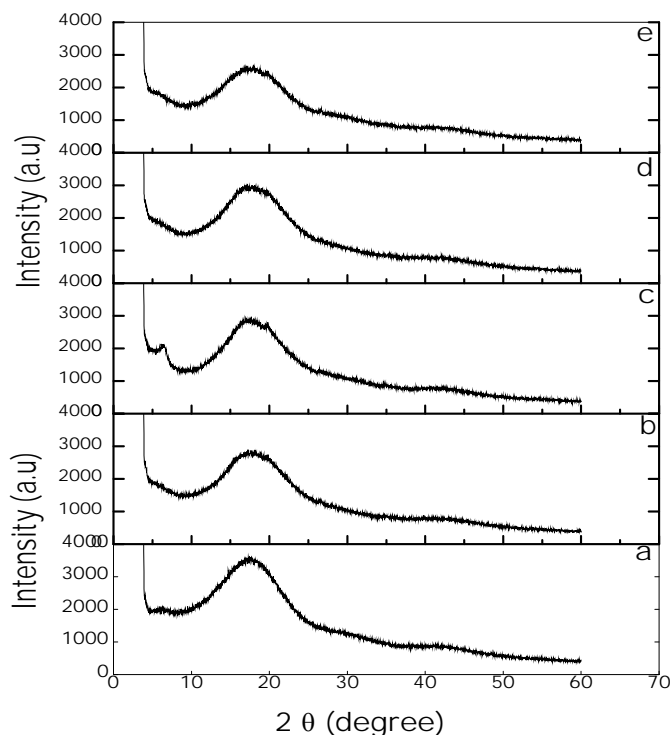


Figure 2. XRD profiles of; (a) 0%, (b) 2.5 %, (c) 5 %, (d) 7.5 % and (e) 10 wt % o-MMT filled vinyl ester green composites

In order to present the results in a better perspective, these results are projected on to a two-dimensional plane using the values of vinyl ester/o-MMT

nanocomposites fitted into an ellipsoid shape with D_s ($2\theta = 17.35^\circ$) in along the x-axis and the other D_s ($2\theta = 42.44^\circ$) in along y-axis. Here 2θ is the angle

between the two (hkl) planes and D_s is the crystal size corresponding to the particular (hkl) reflection. Figure 4

shows a comparison of ellipsoid shapes of crystallites of vinyl ester/o-MMT/TS nanocomposites.

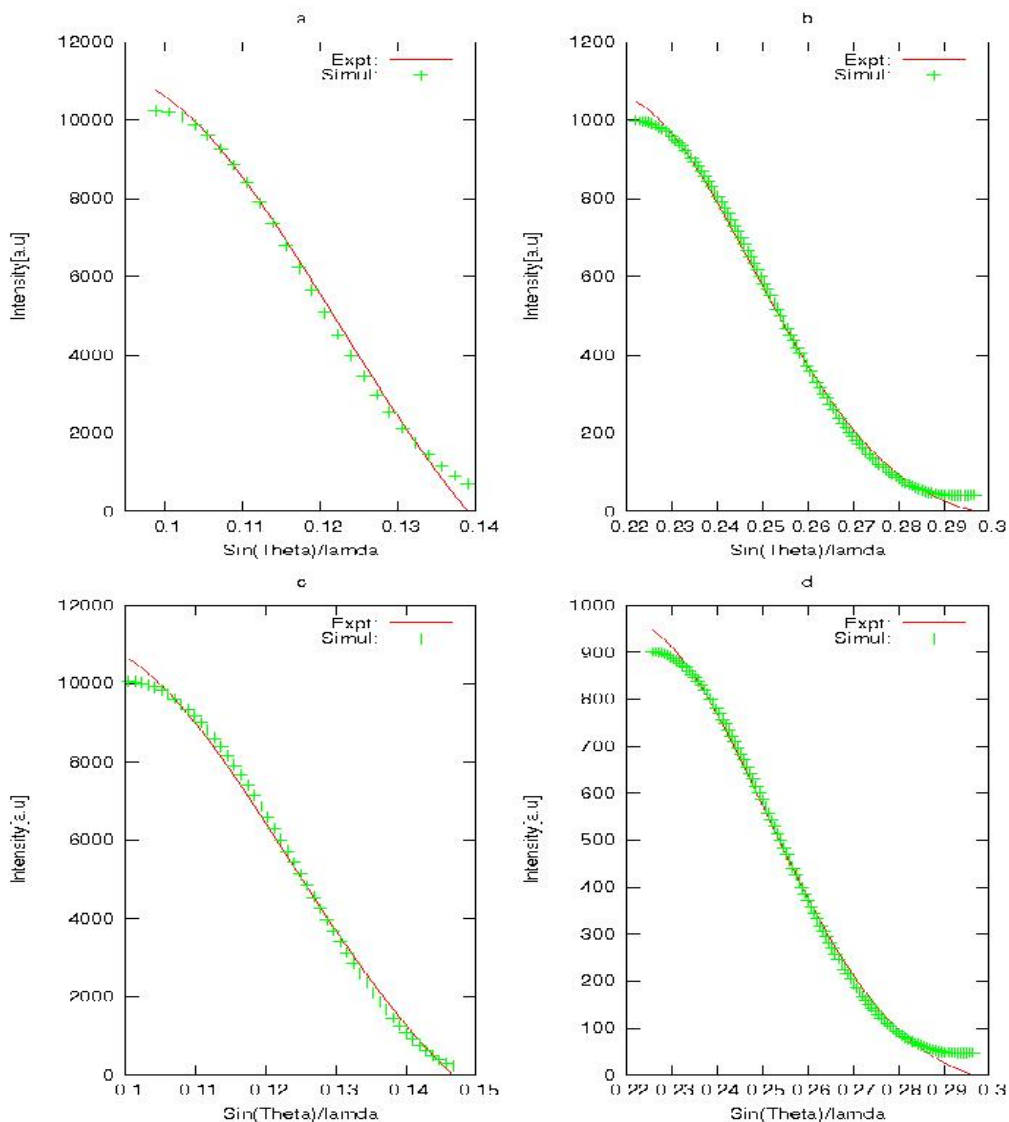


Figure 3. Experimental (+++) and simulated (---) intensity profiles of prominent x-ray reflection obtained using exponential distribution function for (a) 0 %, (b) 5 %, (c) 7.5 % and (d) 10 wt % TS filled nanocomposites

The measured strain (%) and average size (D) in Å of neat vinyl ester and vinyl ester/o-MMT/TS green

composites are given in Table 3. There was a significant change in the strain (%) and average size (D_s) in Å with o-

MMT content. The measured strain (%) and average size (D) in Å lies in the range of 0.1-3.9 and 6.34 - 7.71 respectively. From Table 3, it was found that 10% TS loaded Nano composite exhibit higher value of strain (%) and average size. The variation in number of unit cells (<N>) and D_s values with filler content can be associated with co-operative

movements of the molecular chains that form the amorphous region at interfacial regions. Such movements trigger the motions in the crystalline phase, which result in increase in the number of unit cells (<N>) and D_s values. This is in agreement with the observations made by earlier investigations for entirely different class of materials [22].

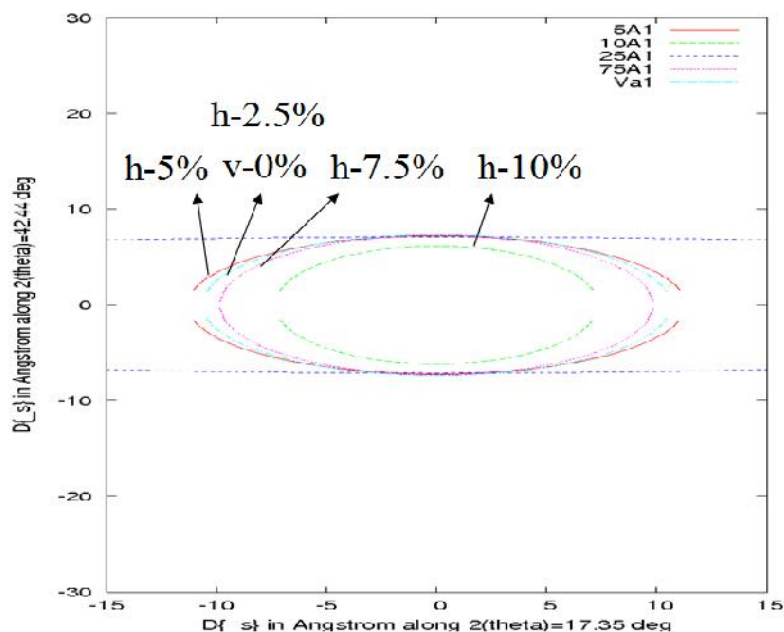


Figure 4. Ellipticity of crystallites observed in nanocomposites

Table 3. Microstructural parameters calculated using Williamson-Hall (W-H)

TS content in resin	Strain (%)	Average size (D) in Å
0	1.20	7.71
2.5	0.40	7.06
5	1.50	6.34
7.5	0.10	6.45
10	3.90	7.45

The surface weight and number of unit cells obtained from the x-ray profile for all the samples were compared with the corresponding tensile strength and are shown in Figures 5 (a)–(b). From the figure, it was noticed that the variation in tensile strength strongly depends on the

surface weight and number of unit cells of the hybrid nanocomposites. It was also evident from the figure that there was no approximate linear relationship between surface weight, number of unit cells and tensile behavior of the composites.

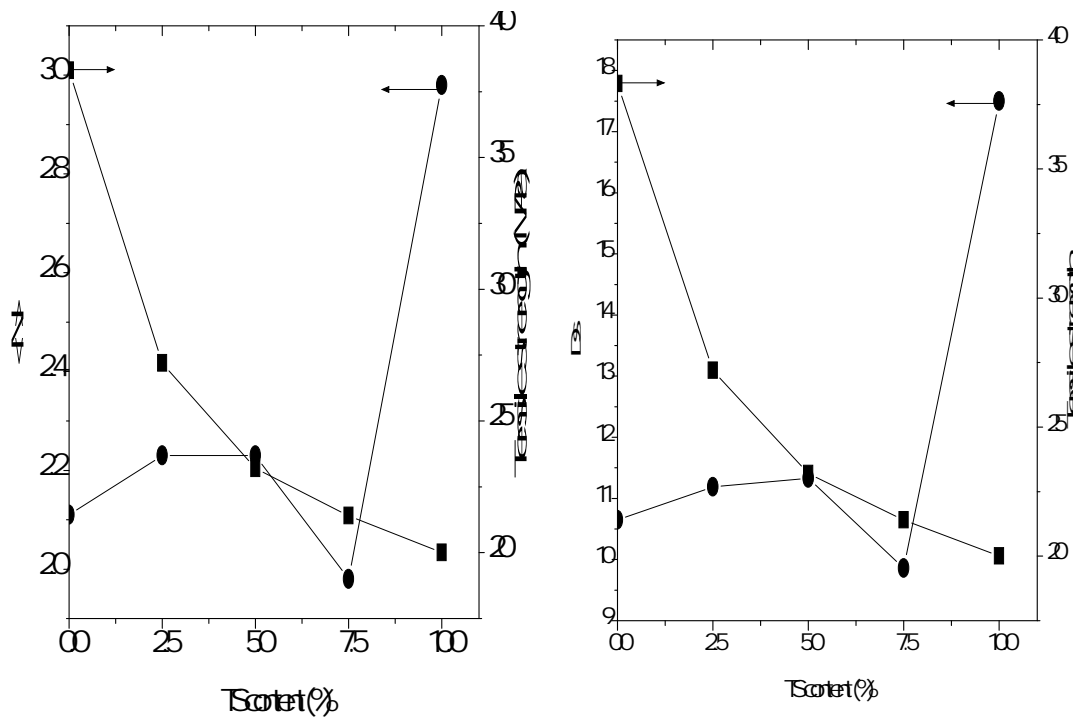


Figure 5 (a-b). Effect of TS concentration on tensile strength, surface weight and number of unit cells of vinyl ester hybrid nanocomposites

Conclusion

Economical and ecological concern is driving the whole world to produce cost-effective and eco-friendly green composites. It was noticed that, the bare vinyl ester and TS filled vinyl ester hybrid nanocomposites showed good resistance to acids. Percentage swelling

in hexane media of bare vinyl ester is high as compared to filled vinyl ester hybrid nanocomposites. This result clearly indicates that resistance to the organic solvents increases with decrease in TS content in vinyl ester matrix. All the composites showed uptake of water which increases with

increase in filler content and are attributed to the presence of lignocellulosic TS filler in the green composites. The interplanar (d_{hkl}) distances of the first and second main peaks lie in the range of 4.98-5.25 and 2.12-2.25 respectively. The d_{hkl} values of the composites indicate a slight variation. There was broad and major peak in the 2θ region $17.35 - 17.79^\circ$ and a small shoulder in the 2θ region around $40.00 - 42.44^\circ$. It is evident from the figure that with increase in o-MMT content, the peak shape and size in the 2θ region varied. It was found that, 10% TS loaded nanocomposite exhibits higher value of strain (%) and average size. We have quantified the changes observed from WAXS studies of nanocomposites in terms of crystal imperfection parameters like crystal size and lattice strain and there is one-to-one correspondence with the changes in physical parameters and hence, establishing the structure property relation in these materials.

References

- [1] E. Zini, M. Scandola, *Polymer Composites*, **2011**, 12, 1905–1915.
- [2] S.H.P. Bettini, M.P.P. M. Josefovich, C. Lotti, *Proceedings of the Polymer Processing Society 26th Annual Meeting, PPS-26, Banff, Canada*, **2010**, 4-8.
- [3] B.C. Bonse, M.C.S. Mamede, R.A. da Costa, S.H.P. Bettini, *Proceedings of the Polymer Processing Society 26th Annual Meeting, PPS-26, Banff, Canada*, July **2010**, 4-8.
- [4] S. Kalia, B.S. Kaith, I. Kaur, *Polymer Eng. Sci.*, **2009**, 49, 1253-1272
- [5] B.C. Suddell, W.J. Evans, *Taylor & Francis Group, Florida*, **2005**, 9, 237–297
- [6] A. R. Sanadi, D. F. Caulfield, R. M. Rowell, *Plastics Eng.*, **1994**, 50, 27-28
- [7] J. D. Ambrósio, A. A Lucas, *Polymer Composites*, **2011**, 32,5, 776-785.
- [8] Sh. Pashaei, S. Hosseinzadeh, *Iran. Chem. Commun.*, **2016**, 4, 102-114.
- [9] R.A. Sheldon, J. Dakka, *Manufacturing Chemist, Chem., Ind. (London)*, **1992**, 7, 127-133.
- [10] S. Pashaei, Siddaramaiah. A. Ahmed Syed. *Polym.-Plast. Tech. Eng.*, **2011**, 50, 1187–1198.
- [11] R.B. Prime, E.A. Turi, Ed., *Academic, New York*, **1981**, 5, 532-547.
- [12] H. Kiao, Z.H. Ping, J.W. Xe, T.Y. Yu, *J. Polym. Sci., Part A Polym. Chem.*, **1990**, 28, 585-594.

- [13] P. Parameswara, T. Demappa, T. Guru Row, R. Somashekar, *Iran. Polym. J.* **2008**, *17*, 821-826.
- [14] K. A. Omnell, J. E. Glas, *J. Ultrastruct. Res.* 1960,*3*, 334-338.
- [15] H. Somashekarappa, V. Annadurai, G. Subramanya, R. Somashekar, *Mat. Lett.* **2002**, *53*(6), 415-420.
- [16] V. K. Smitha, R. Gopalkrishne, S. S. Mahesh, N. G. Malleshi, R. Somashekar, *Int. J. Food Prop.*, **2008**, *11*(4), 781-785.
- [17] R. K. Nandi, K. Kuo, W. Schlosberg, G. Wissler, J. B. Cohen, B. Crist, Jr., *J. Appl. Crystallogr.* **1984**, *17*(1), 22-27.
- [18] W. L. Smith, *J. Appl. Crystallogr.* **1972**, *5*, 127-132.
- [19] T.G. Rials, M.P. Wolcott, *J. Mater. Sci. Let.*, **1998**, *17*(4), 317-319.
- [20] T. Jeevananda, Siddaramaiah, V. Annadurai, R. Somashekar, *J. Appl. Polym. Sci.*, **2001**, *82* (2), 383-388.
- [21] W.J. Choia, Se Hoon Kimb, Y.J. Kim, S. Chul Kim, *Polymer*, **2004**, *45* (17), 6045-6057.
- [22] R.L. Shogren, Z.S. Petrovic, Z.Liu, S.Z.Erhan, *J. Polym. Environ.*, **2004**,*12* (3), 173-178.